Effect of secondary additives on the properties of vanadium-aluminum mixed oxide catalysts used in the oxidation of propane

Víctor G. Baldovino-Medrano,[1,2,3*] *Benjamin Farin,*[3] *Eric M. Gaigneaux*[3,*].

[1]Centro de Investigaciones en Catálisis -CICAT-UIS (CICAT), Parque Tecnológico de Guatiguará, Universidad Industrial de Santander, km 2 vía El Refugio, Piedecuesta, 681011, Colombia.

[2]Laboratorio de Ciencia de Superficies (Csss_UIS), Parque Tecnológico de Guatiguará, Universidad Industrial de Santander, km 2 vía El Refugio, Piedecuesta, 681011, Colombia.

[3]Institute of Condensed Matter and Nanosciences - IMCN, Division Molecular Chemistry, Materials and Catalysts –MOST, UCLouvain, Place Louis Pasteur 1, box L4.01.09, B-1348 Louvain-la-Neuve, Belgium.

KEYWORDS. Technical catalysts, tableting, vanadium-aluminum mixed oxide, additives, propane oxidation.

ABSTRACT. We investigated how secondary additives for tableting vanadium-aluminum mixed-oxides affect the mechanical resistance, surface chemistry, and catalytic performance in propane oxidation of tablets based on this material. The secondary additives were magnesium oxide, silica, boron nitride, sepiolite, and zinc oxide while graphite was used as the primary shaping agent. Our results showed that the changes in mechanical strength and porosity were directly related to the softness and ductility of the secondary additive. Overall, we learned that when manufacturing catalyst tablets, there is a compromise between mechanical strength and loss in mesoporosity and surface area. On the other hand, the components of the formulated tablets did not show signs of establishing a chemical interaction with the vanadium-aluminum mixed oxide. Therefore, the effects of the additives that we found on the catalytic performance were ascribed to the fact that the selected secondary additives may act as co-catalysts during propane oxidation. In this sense, boron nitride and sepiolite were best for promoting both the reactivity of the catalytic formulations while showing a better productivity of propene. The data was interpreted suggesting that the promotion effect may be due to the combination of a redox mechanism over the vanadium-aluminum mixed oxide phase and to a surface radical mechanism occurring over the active moieties of these secondary additives.

1. INTRODUCTION

Shaping is a must for technical catalysts and its importance cannot be overstated.[1–16] As Armor pointed out in his 2005 essay: Do you really have a better catalyst?,[16] “It is important to remember that there is an overall rate (of reaction) determined by catalyst composition, catalyst shape/structure, porosity, and additives; sometimes an extremely active powder may be difficult to formulate into a commercial product which fits the reactor conditions.” Therefore, technical catalysts are shaped bodies that possess the catalytic functionalities needed for high cost-effective processes and that have adequate qualities for fitting specific reactor types, configurations, and conditions.[1–16] To fulfill these requirements, they have to possess convenient composition, size, geometry, and porosity that provide mechanical resistance, thermal, and chemical resilience. When a promising catalyst powder is identified in the laboratory, the scaling-up of its production includes designing a series of unit operations for shaping it. The shaped catalyst is what is called the technical catalyst.

The catalytic powder is often combined with other substances that may serve as binders, lubricants, plasticizers, compaction agents, porogeneous agents, and other additives promoting chemical reactivity or stability during the forming operation that leads to shaping.[2,7,9,12,13] The formulation of a technical catalyst hence consists of making an adequate selection of these substances and devising their relative composition in the formulation while keeping in mind the method selected for the forming operation.[2,4,5,11,14,17,18]

Conventional forming operations are spray-drying, granulation, extrusion, and tableting (or pelleting). Extrusion and tableting are most often employed for forming catalysts aimed to processes operated with fixed-bed or trickle-bed reactors at the ton scale; e.g. hydrotreating, reforming, and selective oxidations.[3,12,19] When a technical catalyst is installed within these reactors, its lifespan depends on how it withstands the chemical, thermal, and mechanical stresses imposed by their own weight, the weight of the reactants, and the constantly changing operation conditions of the process.[20–30] The effects of these stresses are intricately interconnected with each other; e.g. thermal stresses may lead to sintering or crystallization that may make the technical catalyst brittle henceforth promoting particle breakage into irregular bodies and fines that cause channeling, hot-spots, and increased pressure gradients to a point where the reactor plugs and the operation must be stopped. In these instances, catalysts extrudates and tablets must offer the highest mechanical resistance possible without strongly compromising the chemical reactivity and the access of the reactants to the catalytically active centers. Where, the accessibility to the active centers of the catalysts is controlled by the porosity of the shaped catalyst.

In recent years, we have devoted efforts to understand the basics behind the extrusion and tableting of catalytic powders used in selective oxidation reactions.[31–35] Particularly, we have investigated how tableting modifies the physicochemical catalytic properties of vanadium-aluminum mixed (hydr)oxide (VAlO) powders used for the oxidative dehydrogenation of propane.[32,34,36] We found that these powders can only be tableted if they are mixed with low loadings of graphite (G), ca. 1.0 wt.%, because this substance is needed as both lubricant and binding agent during the forming operation. The tablets produced with graphite displayed better selectivity to the production of propene as compared to those made solely with the base VAlO powder. Furthermore, an analysis of the spent catalysts showed that graphite does not decompose or burn during the catalytic tests. The latter was a matter of concern for the studied reaction; propane oxidation. Indeed, Stiles[13] strongly warned upon the risks of graphite burning or oxidation at high temperatures on the stability and performance of industrial catalysts. Unfortunately, and as it is common for literature concerning the shaping of catalysts, the author neither provided evidence to support his warning nor did he mention literature references documenting the fact.

Given the advances described above, we decided to broaden the scope of our research by investigating the effect of putting secondary additives of different acid-base characteristics into the formulation of tablets of VAlO-G over some of the relevant physicochemical and catalytic properties of these materials. For this purpose, we arbitrarily added 5.0 wt.% of the following substances during tableting: basic MgO, neutral or slightly basic sepiolite,[37] neutral boron nitride, neutral or slightly acidic SiO_2, and amphoteric ZnO. The produced tablets were analyzed in terms of their mechanical resistance, porosity, surface chemical composition, and their catalytic behavior on the oxidation of propane. For the latter, we investigated how the produced formulations behaved in front of changes of the reaction temperature and of the O_2/C_3H_8 molar ratio of the reaction feed.

2. EXPERIMENTAL METHODS

2.1. Synthesis of vanadium-aluminum mixed hydroxides

The synthesis of vanadium–aluminum mixed hydroxides in the 1 kg scale was described in detail in previous works.[32–34,38,39] Briefly, adequate quantities of ammonium metavanadate (NH_4VO_3, Isochim, technical degree) and aluminum nitrate nonahydrate ($Al(NO_3)_3 \cdot 9H_2O$, Merck, 95%) were dissolved in distilled water at 333 K in an 80 L stainless steel precipitation tank stirred with a boat propeller type stirrer. A nominal bulk molar V/Al ratio of 0.25 was fixed for the synthesis. The coprecipitation of the mixed hydroxide proceeded at a pH of 5.5. This pH was reached and maintained by adding NH_4OH (Merck, 25%). The obtained hydroxide slurry was filtered in a belt-filter and then washed overnight under stirring with hot water in the co-precipitation reactor vessel. After a second filtration, the recovered solid was dried in a static air stove at 333 K. The dried vanadium–aluminum mixed hydroxide powder was grounded and sieved to particle sizes below 100 μm.

2.2. Tableting

The sifted vanadium–aluminum mixed hydroxide powder was mixed with 1.0 wt.% graphite (Merck, technical grade) and 5.0 wt.% of the selected secondary shaping additives inside a glass bottle.[32,34] These additives were powders of magnesium oxide -MgO: basic- (Aldrich), sepiolite -$Mg_4Si_6O_{15}(OH)_2 \cdot 6H_2O$: neutral or slightly basic-[37] (Sigma-Aldrich), boron nitride -BN:

neutral- (Sigma-Aldrich), silica -SiO_2: neutral or slightly acidic- (Merck), and zinc oxide -ZnO: amphoteric- (Merck), that were all technical grade products. Cylindrical tablets with dimensions: L = 2.3 mm × Ø = 5.1 mm, were manufactured with a hand-operated machine (Ateliers Ed. Courtoy, series 796).[32,34] Tablets were roasted inside a stove under static air at 773 K for 4 h. The formed materials were named following the nomenclature: VAlO-G-Additive. Where, G stands for 1.0 wt.% graphite and Additive was replaced by the corresponding nomenclature adopted for each additive. Namely, Mg = magnesium oxide, BN = boron nitride, Si = silica, Sep = sepiolite, and Zn = zinc oxide.

2.3. Assessment of the physicochemical properties of the materials

Mechanical resistance

The axial compressive strength (σ_ε) of the tablets was measured with an automatic Instron 5566 testing using the methods reported elsewhere.[31,32,34] Tablets were placed in the instrument where they were submitted to an axial load at a constant speed of 5 mm/min. The accuracy of the measured force was ±1 N. The measurements were replicated at least five times for each tested sample.

Surface area and porosity

N_2 adsorption-desorption isotherms at 77 K were measured by the volumetric method in a Micromeritics Tristar 3000 apparatus. The analysis was performed on particles of sizes ranging between 100 and 350 μm. These particles were recovered after crushing the corresponding VAlO-G-Additive tablets. In general, 0.15 - 0.25 g of sample were outgassed overnight at 423 K under a vacuum pressure of 15 Pa before running the analyses. During each test, both the warm and cold free spaces of the sample cells were automatically measured by the apparatus. The relative pressure

(P/P_0) range of the measurements was comprised between 0.01 – 0.99 with ~59 points being collected to complete the isotherms.

X-Ray photoelectron spectrometry (XPS)

XPS measurements were performed with an SSI-X-probe (SSX-100/206) photoelectron spectrometer (Surface Science Instruments) equipped with a monochromatic microfocused Al Kα X-ray source (1486.6 eV) using the same procedures reported elsewhere.[31–34] Sample preparation consisted of crushing and grounding randomly selected tablets into fine powders. These powders were then pressed into small stainless-steel troughs and mounted on a multi-specimen ceramic carrousel used as the sample holder. Samples were then introduced in the preparation chamber of the instrument where they were outgassed overnight over vacuum. Afterward, they were passed to the analysis chamber of the instrument where the pressure was around 1.3×10^{-6} Pa. An area of approximately 1.4 mm^2 (1000 μm x1700 μm) was analyzed for each sample. To avoid issues with sample charging, a Ni grid was placed 3 mm above the carousel holding the samples and the samples were flooded with low energy electrons using a flood gun operated 8 eV. During the analyses, general survey spectra were recorded using a pass energy of 150 eV. Under such a condition, the full width at half maximum (FWHM) of the Au $4f_{7/2}$ peak of a clean gold standard sample was about 1.6 eV. Besides the general spectra, narrow scans were recorded for selected regions of the spectra by setting the pass energy at 50 eV. The stability of the surface charge of the samples during the measurements was monitored by recording the C 1s peak of the samples at the beginning and at the end of the measurements. The recorded data were analyzed with CasaXPS® (Casa Software Ltd., UK) using a Gaussian/Lorentzian (85/15) product function as line shape after subtraction of a Shirley baseline. Further details on the analysis conditions are given elsewhere.[31,32,34,40,41]

2.3. Catalytic tests

The oxidation of propane was used as a test reaction. Tests were carried out in a U-shaped fixed-bed reactor made of quartz; external diameter of the tube = 0.6 cm; external diameter of the fixed-bed = 1.4 cm, L = 19.1 cm, and provided with a frit to hold the catalyst. Before the tests, the tablets of the catalysts were crushed and the recovered particles were sifted to sizes between 200 and 315 μm. Circa 0.1 g of these particles were diluted in quartz spheres (0.4 g, Dp ≤ 200 μm) and put inside the reactor for testing under plug-flow conditions. The volume of the catalytic bed (catalyst plus quartz spheres) was ca. 1.0 cm^3. The empty space between the entrance and exit of the fixed bed was not filled up. The reactor was provided with a thermowell located at the same height as the catalytic bed. This allowed direct sensing and control of the reactor temperature at the level of the catalytic bed. The temperature was sensed by a K-type thermocouple connected to a conventional PID controller. The tests were made as follows. First, the catalysts were dried for 1 h under nitrogen flow after which the reactants were fed to the reactor. Then, the temperature was consecutively ramped up to 723, 748, and 773 K. The feed consisted of 40 cm^3/min of a mixture of O_2 and C_3H_8 and N_2 as diluent. Tests were made at different O_2/C_3H_8 molar ratios; namely, 2.0, 1.5, 1.0, and 0.67. Technical grade propane, 99.999% purity oxygen and 99.999% nitrogen were used. All gases were provided by Praxair and used as received. Reaction products identification was made with an on-line Varian GC provided with three GC columns and two detectors. A Hayesep column coupled with a Molecular Sieve column and a TCD detector were used to separate and quantify O_2, N_2, CO, CO_2, C_3H_8, and C_3H_6. The presence and quantification of oxygenates were managed through a system composed of one EC-Wax column coupled with an FID detector. Further details of the reaction set-up are presented elsewhere.[31,32] Carbon balances around 100% were achieved for each catalytic test. A standard deviation of 10-15 % was accepted due to the uncontrolled limitations of the experimental set-up. The catalytic performance was assessed in terms of fractional conversions and products yields according to the equations:

$$X_i = \frac{(n_i^0 - n_i^f)}{n_i^0} \text{ ; i = } C_3H_8 \text{ or } O_2 \text{ (Equation 1)}$$

$$y_j = \left(\frac{v_j}{v_{C_3H_8}}\right) \times \frac{n_j^f}{n_{C_3H_8}^0 - n_{C_3H_8}^f} \text{ (Eq. 2); j = } C_3H_6, CO_2, CO, \text{ or other oxygenated}$$

hydrocarbons (Equation 2)

3. RESULTS AND DISCUSSION

3.1 Physicochemical properties. First, we will discuss the effect of the use of the selected secondary additives on the mechanical resistance of the materials. Then, we will show that the original mesopore structure of the vanadium-aluminum mixed oxides was kept by tableted materials even though the number of mesopores was reduced by the forces exerted during the forming operation. The latter translated into losses of specific surface area and pore volume which were found to vary with the type of secondary additive.

Mechanical resistance. Figure 1 shows boxplots comparing the axial compression strength for samples of the manufactured tablets. Raw data can be found in **Table S1**. Clearly, the addition of silica, **VAlO-G-Si**, strengthened the axial compression resistance of the tablets beyond the levels reached with the sole addition of graphite, **VAlO-G**. However, the mechanical resistance of **VAlO-G-Si** was highly variable with some tablets having a similar mechanical resistance than those produced with the other secondary additives. To this respect, compared to **VAlO-G**, boron nitride, magnesium oxide, sepiolite, and zinc oxide lowered the mechanical resistance of the manufactured tablets to a very similar extent. In the case of boron nitride, sepiolite, Mohs hardness ~ 2.0 for both, and zinc oxide, Mohs hardness ~ 4.5, these are soft materials that could have been expected to lower the mechanical resistance of the tablets. In the cases of magnesium oxide and silica, these are both hard solids, Mohs hardness ~ 5.5 and 7.0,[42] respectively, but, as mentioned before, only silica enhanced the mechanical resistance beyond the values obtained for the tablets made with graphite. Although, the tablets manufactured with magnesium oxide had the highest median axial compressive strength, ~35 MPa, among those made with the other additives. We do not know the reason (or reasons) behind these trends at this point. One may suppose though that they are related to the changes in the hardness of the secondary additives commented before. According to the literature,[14,17,43] refractory oxides make tableting very difficult since their hardness makes them less ductile. Ductility is necessary for wielding the particles from the different substances formulated to make the technical catalyst via tableting.[14,17,43]

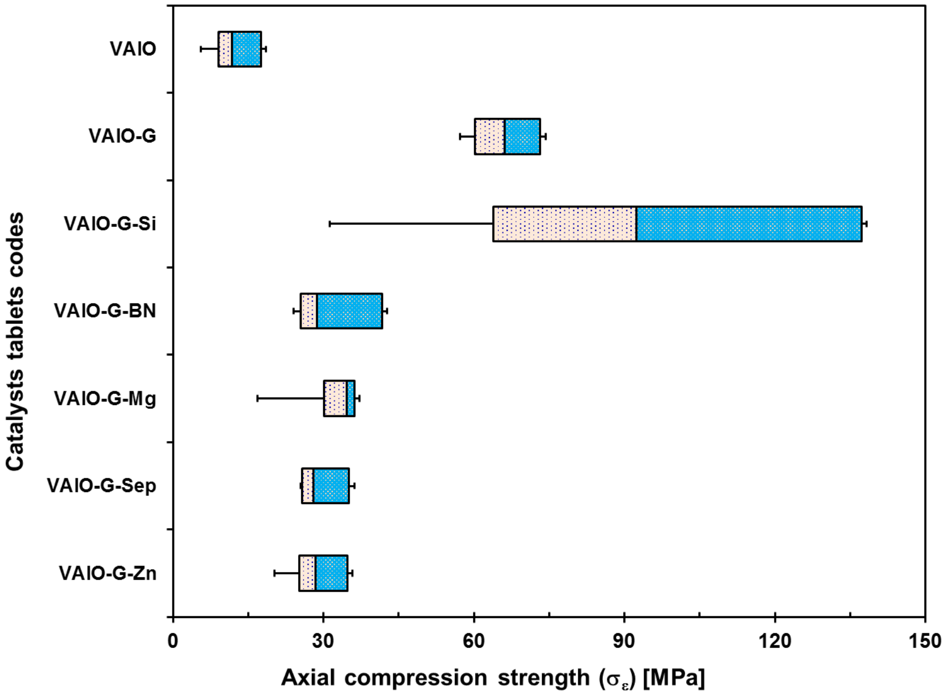

Figure 1. Boxplots for the mechanical resistance of vanadium-aluminum mixed tablets manufactured with different shaping additives. Nomenclature: VAlO-G-Additive, where, G = 1

wt.% graphite, Si = SiO_2, BN = Boron nitride, Mg = Magnesium oxide, Sep = Sepiolite, Zn = Zinc oxide. All tablets contained 5.0 wt.% of the corresponding additives.

Porosity. Figure 2 shows two nitrogen physisorption isotherms, selected among those measured for the manufactured catalysts tablets, that illustrate that the mesoporous structure of the catalytic vanadium-aluminum mixed oxide was kept by the tablets made with the secondary additives. The isotherms, measured with particles recovered after crushing tablets of the vanadium-aluminum mixed oxide and of the formulation with 1.0 wt.% graphite and 5.0 wt.% silica, are presented in terms of a χ-plot.[44,45] We used this method because for the present materials it is more adequate for estimating surface area, $SA\chi$, than the conventional BET method.[46] As we discussed in a previous contribution,[32] vanadium-aluminum mixed oxide powders consist of platy particles making slit-like mesopores that produce type II isotherms with an H3 hysteresis loop. As the results presented in **Figure 2** show, our tests did not detect changes of the pore structure after tableting using the additives studied herein. This is further corroborated by the results of the BJH calculations[47] done for assessing the corresponding mesopore size distributions, Insets **Figure 2** and **Figure S2**.

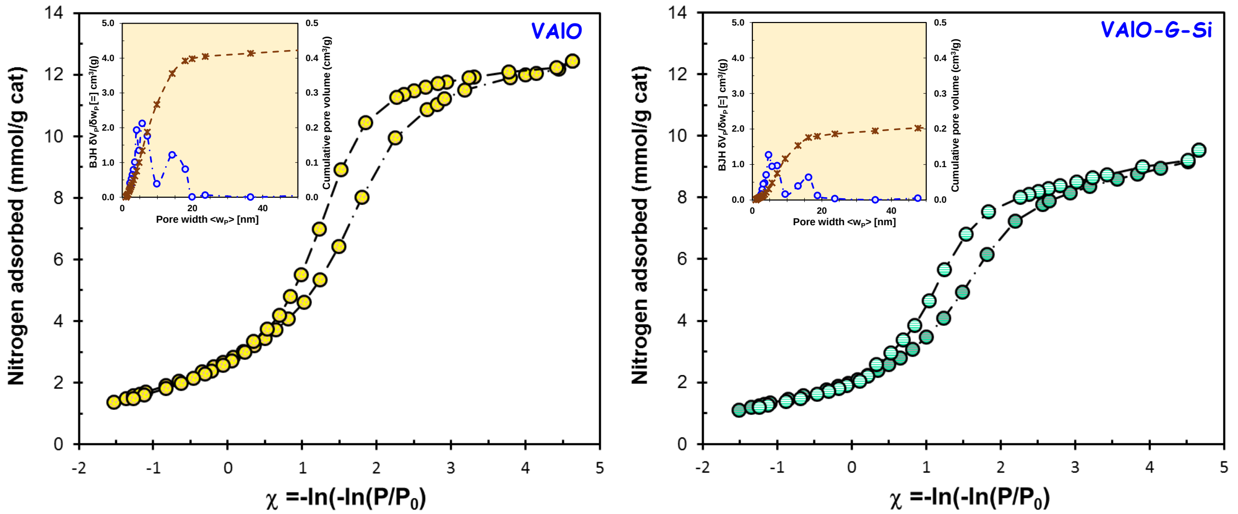

Figure 2. Representative nitrogen physisorption isotherms, χ-plots,[32,44] for particles recovered from two representative formulations of vanadium-aluminum mixed oxide tablets:

VAlO = vanadium-aluminum mixed tableted without additives. **VAlO-G-Si** = vanadium-aluminum mixed tableted with 1.0 wt.% graphite and 5.0 wt.% silica. Physisorption isotherms for the other manufactured tablets can be found in **Figure S1**. Insets correspond to BJH[47] pore size distributions and cumulative pore volumes considering slit-shape pores. Other pore size distributions and cumulative pore volume plots are presented in **Figure S2**.

Indeed, the original two families of mesopores found for the vanadium-aluminum mixed oxide powder after tableting; one around 6.0 nm and the other around 15 nm, were also found for the powders recovered from the other tablets, **Figure S2**. In conclusion, neither of the formulations employed for tableting the vanadium-aluminum mixed oxide catalyst modified its mesoporous structure.

Although the manufactured tablets kept the mesoporous structure of the vanadium-aluminum mixed oxide, tableting led to a loss in the number of mesopores hence decreasing the surface area of the materials. This effect is made patent by the results feature in **Figure 3** (numerical values are reported in **Table S1**). We may notice that, as secondary additives, magnesium oxide and silica roughly had a higher surface area and cumulative pore volume than the tablets produced solely with graphite. One may also notice that the tablets produced with sepiolite were those with the least loss in surface area and cumulative pore volume while keeping the same level of mechanical strength of the tablets manufactured with zinc oxide and boron nitride. The effect of sepiolite may be explained considering that this material is a clay binder whose platy and ductile particles may easily intercalate with those of the vanadium-aluminum mixed oxide. However, its softness does not contribute to enhancing the mechanical resistance of the tablets. Similar considerations can be made for explaining the effects of boron nitride and zinc oxide who are also soft layered materials.

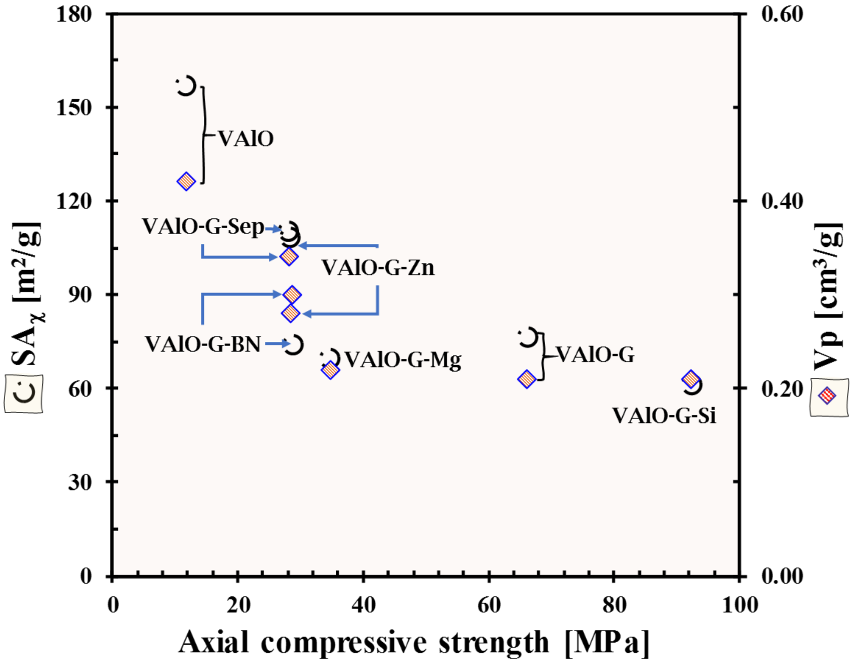

Figure 3. Surface area, SAχ, and cumulative pore volume, V_p, plotted as a function of the median of the axial compressive strengths exhibited by the manufactured tablets. Nomenclature: VAlO-G-Additive, where, G = 1 wt.% graphite, Si = SiO_2, BN = Boron nitride, Mg = Magnesium oxide, Sep = Sepiolite, Zn = Zinc oxide. All tablets contained 5.0 wt.% of the corresponding additives.

In summary, we found that the use of the secondary additives for tableting vanadium-aluminum mixed oxides has a strong impact on the mechanical resistance of the manufactured tablets. Specifically, if the additive is a refractory solid such as silica, the produced tablets increase their mechanical strength. Meanwhile, if the additive is soft; e.g. boron nitride, sepiolite, zinc oxide, the mechanical strength of the tablets decreases. In general, tableting, as practiced under the conditions of the present study, does not alter the mesoporous structure of the catalytic powder. What tableting does make nonetheless is to reduce the number of mesopores of the catalyst. This translates into losses in surface area and pore volume. In this sense, softer additives mitigate such losses but at the above-mentioned expense in mechanical strength. This teaches us that the mechanical resistance of a catalytic tablet cannot be optimized without reaching a compromise between this property and surface area.

We are going to discuss now how the secondary additives of the catalyst tablets affected surface chemistry as measure by XPS.

Surface chemistry. Table 1 shows the surface composition of particles recovered after crushing the manufactured tablets. The presented composition is representative of the internal surface of the tablets which may differ from what is present at their external surface.[21,32] The internal surface of the tablets is where most of the active sites of the catalyst are located though. Therefore, its characterization is relevant for understanding catalysis; particularly, at the laboratory scale, which is the present case, where transport limitations are ruled out.[32] The first thing to comment about these results is that the composition of the tablets made from the vanadium-aluminum mixed oxide without and with graphite, **VAlO** and **VAlO-G**, respectively, are similar to what we reported in our previous contribution.[32] Namely, the molar percentage of vanadium, ~4.0 mol%, and the V/Al molar ratio, ~0.16, of these catalysts are within the range of values found earlier.[32] Besides, the V^{5+}/V^{4+} molar ratio of this set of materials was also within the margins of what has been found earlier for vanadium-aluminum mixed oxides.[48]

Table 1 Elemental surface composition of particles recovered after crushing the manufactured tablets measured by X-Ray photoelectron spectroscopy. Nomenclature: VAlO-G-Additive, where, G = 1 wt.% graphite, Si = SiO_2, BN = Boron nitride, Mg = Magnesium oxide, Sep = Sepiolite, Zn = Zinc oxide. All tablets contained 5.0 wt.% of the corresponding additives.

Catalyst code	**Element mole%**				
	C	O **Organic**/**Inorganic**	V **V^{5+}/V^{4+}**	Al	Others
VAlO	14.0	**4.7**/**50.6**	4.6 **2.8**	25.8	N = 0.3
VAlO-G	19.7	**4.2**/**47.0**	3.5 **2.5**	25.3	N = 0.4
VAlO-G-Si	20.6	**3.9**/**51.7**	2.3 **2.8**	11.0	Si = 10.5
VAlO-G-BN	21.4	**4.7**/**32.0**	2.8 **2.1**	13.9	B = 12.5 N = 12.8
VAlO-G-Mg	27.4	**5.6**/**42.8**	3.1	16.1	Mg = 5.0

			4.7		
VAlO-G-Sep	24.5	5.1/46.2	3.6 2.3	17.6	Si = 1.8 Mg = 1.3
VAlO-G-Zn	26.6	4.4/44.5	3.5 2.9	16.4	Zn = 4.7

We want to discuss now how the concentration of surface carbon increased with the addition of the secondary additives during tableting. Surface carbon has two sources in the featured materials; carbon from graphite, that roughly contributes 5.0 mole%, and adventitious carbon[49–51] adsorbed from the environment which roughly contributes 14.0 mole% in the case of VAlO materials, **Table 1** and previous works.[32] What seems interesting from the current results is how the concentration of carbon increased for the tablets made with magnesium oxide, 27.4 mole%, sepiolite, 24.5 mole%, and zinc oxide, 26.6 mole%, while it rather remained at the same level for the tablets made with silica, 20.6 mole%, and boron nitride, 21.4 mole%. These increments are due to an increase in adventitious carbon since the loading of graphite was the same in all cases. Considering this fact, a correlation between the concentration of surface carbon and the acidobasicity of the additives is suggested. We may notice that both silica and boron nitride, which are rather neutral, did not enhance carbon concentration while basic MgO, slightly basic sepiolite, and amphoteric ZnO did. Therefore, the concentration of adventitious carbon can be employed as an indirect marker for the acidobasicity of the materials. One may recall that the surface of metallic oxides tends to minimize its surface energy by adsorbing organic molecules with lower surface tension.[52] This observation will become handy when analyzing the general catalytic trends found herein, Section **3.3**.

We now focus on the concentration of oxygen. We discriminated the total concentration of this element into organic and inorganic simply by subtracting the oxygen associated to the C 1s peak from the concentration of oxygen calculated with the O 1s peak (see **Table S3** and **Figure**

S3 for details). Such a distinction is important because only inorganic oxygen will play a role in catalysis since organic carbon is weakly bonded to the surface hence being eliminated during the drying stage of the catalytic tests. Assuming the stoichiometries of the additives, we may further aim distinguishing the oxygen that should belong to the vanadium-aluminum mixed oxide from the oxygen that belongs to the additives. For this, we will assume that the added oxides obey their nominal stoichiometries, accepting that this is a rough approximation. Therefore, silica will be SiO_2, magnesium oxide will be MgO, zinc oxide will be ZnO, and sepiolite will follow the empirical formula accepted in mineralogy: $Mg_4Si_6O_{15}•6(H_2O)$.[53] For sepiolite, it can be noticed that the Si/Mg measured by XPS, 1.8/1.3 ~ 1.4 is approximately the same as the one of the mineral, 6/4 = 1.5. According to simple arithmetic, we then have that the mole percentages of oxygen associated to the vanadium-aluminum oxide decrease in the order: VAlO, 50.6 mole% > VAlO-G, 47.0 mole% > VAlO-G-Sep, 39.9 mole% ~ VAlO-G-Zn, 39.8 mole% ~ VAlO-G-Mg, 37.8 mole% > VAlO-G-BN, 32.0 mole% ~ VAlO-G-Si, 30.7 mole% . Two facts can be highlighted from such a comparison: (i) both graphite and the secondary additives reduced the concentration of surface oxygen linked to the catalytic phase. Where, the secondary additives further decreased the concentration of such oxygen. (ii) The additives with neutral acidobasicity, boron nitride and silica, showed the lowest concentration of oxygen linked to the vanadium-aluminum mixed oxide whereas those with acidobasic qualities, sepiolite, magnesium oxide, and zinc oxide, led to similar concentrations of this kind of oxygen. These trends do not correspond to the formation of new bonds between the catalytic phase and the additives since each substance kept their chemical identity after tableting, see Supplementary Information and **Figure S3** and **Table S3**, featuring the analysis of the chemical species of the materials made by XPS. This result is a corroboration on the fact that conventional tableting does not modify the chemical nature of mixed oxides.[31,32]

3.2 Catalytic behavior

We first address how the temperature, at a fixed O_2/C_3H_8 molar ratio = 2/3, modified the catalytic behavior of the formulated tablets and then we will analyze how the O_2/C_3H_8 molar ratio, at a fixed temperature = 723 K, changed the catalytic performance. We will also separate the presentation of the results discussing first the tendencies found for the conversions of propane and oxygen and then the distribution of products. Our analysis will not include rigorous kinetic considerations since the experiments were done under conditions where thermodynamic equilibrium effects cannot be completely ruled out.[54] Such a limitation is justified at this stage of the research since the goal was to identify the main effects that the selected secondary additives have on the overall catalytic behavior.

Effect of temperature on conversion. **Table 2** shows the steady state average conversions of propane and oxygen as a function of temperature for the formulated catalysts. Excepting the catalyst formulated with sepiolite, VAlO-G-Sep, all catalysts started approaching full oxygen conversion at 748 K. Oxygen was the limiting reactant and this set the limit for the conversion of propane. We will limit our comparison of the catalytic performances at the results found at 723 K since an analysis under a full conversion regime would be mostly controlled by thermodynamics. We will also limit our comparisons to the conversion of propane since, under the current conditions, the conversion of oxygen was roughly twice the conversion of the hydrocarbon in all instances. This suggests that, regardless of the nature of additive, the reactions of oxidation of propane were prevalent during the tests. Keeping these considerations in mind, the reactivity of the formulated catalysts decreased in the following order: VAlO-G-Sep ($X_{C_3H_8}$ = 0.40) ≥ VAlO-G-BN ($X_{C_3H_8}$ = 0.37) > VAlO ($X_{C_3H_8}$ = 0.32) > VAlO-G-Zn ($X_{C_3H_8}$ = 0.27) ≥ VAlO-G-Si ($X_{C_3H_8}$ = 0.26) ≥ VAlO-G-Mg ($X_{C_3H_8}$ = 0.23) > VAlO-G ($X_{C_3H_8}$ = 0.19). Two facts can be highlighted from this trend: (i) all secondary additives increased the reactivity of the catalytic formulations as compared to the reference made with graphite, VAlO-G. (ii) The acido-basicity of the secondary additives did not seem to play a crucial role on defining the reactivity of the catalysts as a function of temperature. Indeed, the formulations made with sepiolite, weakly basic, and boron nitride, neutral, were more reactive than the vanadium-aluminum mixed oxide material itself, while the formulations made with more basic MgO, neutral or slightly acidic SiO_2, and Lewis acidic ZnO showed a rather similar reactivity. Beyond such a consideration, as additives, sepiolite and boron nitride promoted the reactivity of the VAlO catalyst.

Concerning the effect of sepiolite on the catalytic behavior, around the mid-90s, Corma et al.[55–58] published a series of studies analyzing the catalytic behavior of vanadium oxides supported on sepiolite and magnesium oxide and concluded that magnesium from these oxides can interact strongly with vanadium if they roasted the magnesium silicate at 923 K before impregnating the vanadium oxide precursor and then roasted again at 823 K. This strong interaction leads to the formation of different vanadium-magnesium mixed oxide phases; MgV_2O_6, $Mg_3V_2O_8$, α- and β-$Mg_2V_2O_7$, that are reactive in propane oxidation. From our current results, we do not have evidence for proving the existence of these interactions. Neither can we compare directly our results to those of Corma et al.[55–58] because they impregnated the vanadium phase over sepiolite while we made a physical mixture between a vanadium-aluminum mixed oxide and the sepiolite additive and then 50 K below the temperature used by Corma et al.[55–58] Therefore, although we are certain that adding sepiolite during the tableting of the vanadium-aluminum mixed oxide catalyst promotes its reactivity, we cannot know still the reasons behinds such a promotion effect.

Regarding the promotional effect of boron nitride, three years after the publication of our results concerning this effect in 2013,[36] the group of Hermans at the University of Wisconsin[59,60] developed research proving that by itself boron nitride is catalytically reactive in alkane oxidations while yielding interesting amounts of olefins. In the specific case of hexagonal boron nitride, this group reported that this material favors parallel alkane cracking reactions instead of their combustion. They further postulated that boron nitride oxidizes to form $B(OH)_xO_{3-x}$ moieties that constitute its catalytically active sites.[61]

One clue towards understanding the effects of sepiolite and boron nitride in our research is to analyze the chemistry measured by XPS, **Tables 1** and **S3**. From these results, we may ask first: did the relative concentration of surface vanadium increased for the formulations made with sepiolite and boron nitride as compared to the base vanadium-aluminum mixed oxide? No, it did not. Therefore, we cannot explain the increase in reactivity by an increase in surface vanadium. This was a general trend, meaning that we did not find a clear correlation between the concentration of surface vanadium and the catalytic performance for any of the materials under any of the studied reaction conditions, **Figure S4**. Second, is the promotion of the reactivity of the catalysts by sepiolite and boron nitride due to a modification on the V^{5+}/V^{4+} ratio of surface vanadium? It might be, but… The V^{5+}/V^{4+} ratio decreased from 2.8 for the vanadium-aluminum mixed oxide to 2.3 and 2.1 in the formulations where sepiolite and boron nitride were added, respectively. However, the VAlO-G formulation showed the same V^{5+}/V^{4+} ratio as VAlO-G-BN and was less reactive. Therefore, we cannot conclude that the promotion of the reactivity of the catalysts is due to a change in the V^{5+}/V^{4+} ratio for these two formulations. Finally, is the promotion related to the quantity of surface inorganic oxygen linked to vanadium? As in the case of the second question, this does not seem to be the case since the relative amount of surface oxygen was mostly at the same level for all catalysts, **Table 1**, but for VAlO-G-BN. Indeed, the catalyst formulated with boron nitride showed the lowest quantity of surface oxygen among the materials, 32.0 mole%.

This suggests that the reactivity of the formulated catalysts is more a matter of the quality and dynamic behavior of the surface oxygen than on its quantity. We further corroborated the lack of correlation between these properties by making boxplots where the catalytic performance is presented as a function of the surface concentration of oxygen linked to vanadium, **Figure S5**.

In general, the negative answers for the three questions asked above show that if we want to understand the chemistry behind the catalytic behavior of multicomponent technical catalysts, we need to consider what would be the individual contribution of each component and how would these components interact among each other and with the reactive surface species. Explaining the behavior of multicomponent catalysts is still an unresolved issue in catalysis science since most investigations are made for understanding model systems. In the past, however, the extensive works of the late Prof. Delmon et al.[62,63] aimed explaining such effects by postulating the so-called remote control theory in which one catalytic phase would be responsible for activating oxygen molecules (or hydrogen) and then spilling it over another catalytic phase. Where, the rate of spillover would determine the reactivity of the system and the dynamics of the reaction. This theory was useful for modelling the kinetic behavior of multicomponent catalysts and reactors.[64–66] More recently, Vuong et al.[67] used an alternative approach for modelling the synergistic effects of mechanical mixtures of catalysts for car exhaust depollution. The approach consisted on making combinatorial kinetics from a library of kinetic models for the individual catalysts that would be physically mixed inside a catalytic reactor. Their work emphasized the role that concentration gradients have on the synergy displayed by mechanical mixtures of catalytic powders. The scope of our present contribution does not comprise an assessment of the above aspects to explain our observations. However, from our results, it seems that they should be considered in future investigations since the conventional analysis of the surface chemistry of the formulations VAlO-G-BN and VAlO-G-Sep failed to provide explanations.

Finally, we want to highlight an index, the reactivity index, that is of interest for technical catalysts used in fixed-bed reactors, **Table 2**. The reactivity index is calculated as the mass of reactant converted per volume of catalyst per hour [$kg_R/(m^3_{-cat} \times h)$]. This index is, of course, analogous to the definition of the so-called Space-Time Yield ($kg_R/(kg_{-cat} \times h)$ used by other authors.[68] Considering that we made our catalytic tests at the laboratory scale and over particles recovered after crushing and sifting catalytic tablets, the values of the reactivity index can be considered as maxima of this index. Results show that formulating the catalyst with graphite decreases the reactivity which means that an industrial unit using the **VAlO-G** formulation will require either a larger volume of catalyst or a higher operation temperature to reach the same level of converted hydrocarbon per volume of catalyst as compared to the tablets made with only the vanadium-aluminum mixed oxide. Conversely, the formulations made with sepiolite and boron nitride would be less catalyst consuming for a process based on these technical catalysts. As already mentioned, besides reactivity, technical catalysts are also assessed in terms of their mechanical strength.[2,9,10,22,28–30] Recalling our results on this property, **Figures 1** and **3** and **Table S1**, the eventual use of tablets formulated with sepiolite and boron nitride in a fixed-bed unit would be a good trade-off between reactivity and mechanical resistance because the latter was higher as compared to the mechanical resistance of the tablets made with the powder of the vanadium-aluminum mixed oxide. Furthermore, as we reported earlier[34] the continuous production of VAlO tablets was impracticable hence the use of graphite or of another type of lubricant is mandatory.[13,69] Another aspect that makes attractive the use of sepiolite and boron nitride as secondary additives for the production of technical catalysts based on the VAlO phase is that they reduce the loss in porosity of the base catalyst, **Figure 3** and **Table S1**. Based on these qualities, both sepiolite and boron nitride are a priori interesting forming additives for technical catalysts used in oxidation processes. In this regard, one must analyze how the secondary additives impact the distribution of products from the oxidation reaction. It is important to keep in mind that, in the case of selective oxidations, a higher reactivity is accompanied by the thermodynamic prevalence of combustion reactions which are, of course, undesirable.

Table 2. Molar fraction conversion of propane and oxygen as a function of temperature, 723, 748, and 773 K, over particles recovered from tablets of the catalytic formulations. Reaction conditions: U-shaped quartz fixed bed reactor, p = atmospheric pressure (Louvain-la-Neuve ~ 1.03 bar), catalyst weight ~ 0.1 g, average diameters of the catalyst particles 315 – 200 μm, catalytic bed volume ~ 1.0 cm^3 (catalyst plus ca. 0.4 g of quartz spheres of diameter ≤ 200 μm), gas flows, F_i [cm^3/min]: $F_{C_3H_8} = 4$; $F_{O_2} = 6$; $F_{N_2} = 30$. Nomenclature: VAlO = vanadium-aluminum mixed oxide; G = 1.0 wt.% graphite; Mg = magnesium oxide; Si = silica; BN = boron nitride; Zn = zinc oxide; Sep = sepiolite. *Reactivity Index (RI) [=] kg$_{\text{Reactant}}$/(m$^3_{\text{-cat}}$×h). -cat = catalyst. For calculating the Vcat in RI, it was assumed that the density of the materials corresponds to the density of the vanadium-aluminum mixed oxide,[33] ρ = 2800 kg/m^3.

Catalyst code	T [K]	$X_{C_3H_8}$	X_{O_2}	$X_{O_2}/X_{C_3H_8}$	RI$_{C_3H_8}$ *	RI$_{O_2}$*
VAlO	723	0.32	0.66	2.04	3983.6	8688.8
	748	0.48	1.00	2.06	5963.1	13178.9
	773	0.50	1.00	2.01	6148.6	13231.9
VAlO-G	723	**0.19**	**0.32**	1.67	**2350.6**	**4211.9**
	748	0.34	0.65	1.93	4156.8	8582.8
	773	0.50	1.00	2.00	6148.6	13192.1
VAlO-G-Mg	723	0.23	0.39	1.72	2808.3	5165.6
	748	0.40	0.78	1.95	4948.6	10317.9
	773	0.51	1.00	1.94	6359.0	13231.9
VAlO-G-Si	723	0.26	0.57	2.18	3229.0	7523.2
	748	0.41	0.87	2.14	5022.8	11523.3
	773	0.50	1.00	2.02	6136.3	13245.1
VAlO-G-BN	723	**0.37**	**0.74**	2.01	**4565.1**	**9814.6**
	748	0.49	1.00	2.04	6049.7	13192.1
	773	0.50	1.00	2.02	6123.9	13231.9
VAlO-G-Zn	723	0.27	0.50	1.85	3352.7	6622.6
	748	0.46	0.94	2.06	5641.4	12450.4

	773	0.50	1.00	2.00	6198.1	13245.1
VAlO-G-Sep	723	**0.40**	**0.84**	2.09	**4948.6**	**11059.7**
	748	0.50	1.00	1.99	6210.5	13245.1
	773	0.51	1.00	1.97	6272.4	13245.1

Effect of temperature on the distribution of products. **Scheme 1** presents a reaction pathway for propane oxidation over the catalytic formulations studied in this work. The scheme was made from the products detected by on-line gas chromatography during the catalytic tests. Accordingly, besides the main reaction products; propene, carbon monoxide and carbon dioxide, five oxygenated hydrocarbons were also produced: 2-methyloxirane, 2-propanone, propanal, 2-propenal, and 1,3,3-triethoxy-1-propene.

Scheme 1. Reaction scheme representing the products found during the catalytic tests. Reaction conditions: U-shaped quartz fixed bed reactor, T = 723 – 773 K, *p* = atmospheric pressure (Louvain-la-Neuve ~ 1.03 bar), catalyst weight ~ 0.1 g, average diameters of the catalyst particles 315 – 200 μm, catalytic bed volume ~ 1.0 cm^3 (catalyst plus ca. 0.4 g of quartz spheres of diameter ≤ 200 μm), gas flows, F_i [cm^3/min]: $F_{C_3H_8} = 4$; $F_{O_2} = 6$; $F_{N_2} = 30$.

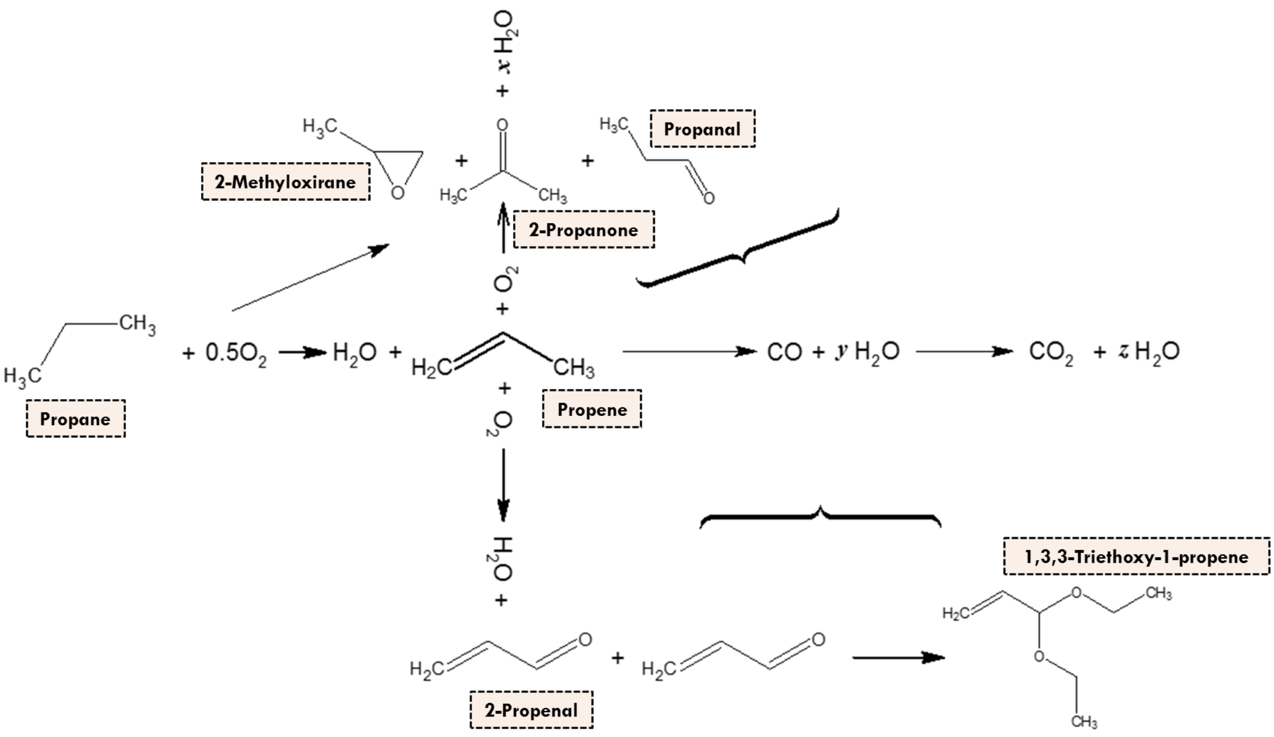

The simultaneous presence of the oxidative dehydrogenation product: propene, combustion products: CO and CO_2, and oxygenates suggests that diverse reaction mechanisms may be operating simultaneously under our conditions. It has been established that, at temperatures below 773 K, propane oxidation may proceed over mixed oxides via a redox mechanism or a surface radical mechanism.[68,70] The redox mechanism comprises the activation of propane into an allylic intermediate over reduced metallic moieties, e.g. $V^{\delta+}$ centers, and the coordination of such kind of reactions with the addition of lattice oxygen to the surface activated complex while gaseous oxygen is activated and thereupon being incorporated to the lattice of the oxide. The unfolding of this type of mechanism in propane oxidation leads to the production of propene if the allylic surface intermediate is rapidly stabilized and desorbed into the gas phase and to the production of CO and CO_2 which are the more stable reaction products. It is interesting to recall that the production of CO has been related to lattice oxygen while the production of CO_2 is related to a high consumption of oxygen by the catalyst, **Table 2** and previous literature reports.[70,71] On the other hand, the surface radical mechanism has been associated to the production of propyl radicals either by Lewis acid centers or by a homolytic scission of a C-H bond of the molecule that leads to propyl and hydrogen radicals. The propyl radical is further oxidized to produce selective oxidation products such as the ones featured in **Scheme 1**.

Table 3 shows the molar yields and the productivity of propene for the catalytic formulations as a function of temperature. Specific values of the molar yields of the oxygenated hydrocarbons are given in **Table S4**, Supplementary Information. We may notice the following: (i) although the productivity of propene over the catalytic formulation made with magnesium oxide was the highest, the yields to propene were very similar among all catalysts and tended to decrease with increasing the temperature. (ii) The production of oxygenates was more important for the formulations made with graphite, magnesium oxide, silica, and sepiolite. For the two first formulations, the increase of temperature did not reduce such a production in contrast to what happened to the latter. (iii) All catalytic formulations tended to produce more CO than CO_2. This tendency was favored by the increase of temperature. As we have already commented, all the catalytic formulations started reaching full conversion of oxygen at 748 K hence limiting the conversion of propane stoichiometrically. Therefore, a kinetic discussion of the tendencies enumerated above is aimless because the reaction is strongly influenced by thermodynamics. However, the behavior of the catalysts in the reactions is not solely determined by thermodynamics but also in part by kinetic effects linked to the chemistry of the catalytic phases that are present in each formulation.

Table 3. Molar yields (y_j) from propane oxidation as a function of temperature, 723, 748, and 773 K, over particles recovered from tablets of the catalytic formulations. Reaction conditions: U-shaped quartz fixed bed reactor, p = atmospheric pressure (Louvain-la-Neuve ~ 1.03 bar), catalyst weight ~ 0.1 g, average diameters of the catalyst particles 315 – 200 μm, catalytic bed volume ~ 1.0 cm^3 (catalyst plus ca. 0.4 g of quartz spheres of diameter ≤ 200 μm), gas flows, F_i [cm^3/min]: $F_{C_3H_8}$ = 4; F_{O_2} = 6; F_{N_2} = 30. Nomenclature: VAlO = vanadium-aluminum mixed oxide; G = 1.0 wt.% graphite; Mg = magnesium oxide; Si = silica; BN = boron nitride; Zn = zinc oxide; Sep = sepiolite. *y_{Oxy} : yield to oxygenated hydrocarbons = sum of the yields of 2-methyloxirane, propanal, 2-propanone, 2-propenal, 1,3,3-triethoxy-1-propene. ☼Propene and Oxygenates Productivity Index (PI) [=] kg$_{C_3H_6}$ or kg$_{Oxy}$/(m^3$_{-cat}$×h). -cat = catalyst. For calculating the V_{cat} in PI, it was assumed that the density of the materials corresponds to the density of the vanadium-aluminum mixed oxide,[33] ρ = 2800 kg/m^3.

Catalyst code	T [K]	y_{CO_2}	y_{CO}	y_{CO}/y_{CO_2}	$y_{C_3H_6}$	y_{oxy}*	$PI_{C_3H_6}$	PI_{Oxy}
VAlO	723	0.11	0.13	1.18	0.08	2.34E-04	978.0	3.8
	748	0.14	0.26	1.86	0.08	4.85E-04	952.9	7.9
	773	0.14	0.29	2.08	0.07	5.70E-04	854.0	9.2
VAlO-G	723	0.06	0.05	0.85	0.07	2.11E-03	856.2	38.1
	748	0.11	0.14	1.19	0.08	3.29E-03	953.2	63.0
	773	0.17	0.26	1.52	0.07	3.05E-03	783.1	63.2
VAlO-G-Mg	723	0.09	0.05	0.55	**0.09**	8.27E-04	**1082.1**	**17.9**
	748	0.17	0.13	0.74	**0.10**	1.98E-03	**1212.0**	**37.6**
	773	0.18	0.24	1.34	**0.09**	1.83E-03	**1010.9**	**41.4**
VAlO-G-Si	723	0.13	0.07	0.51	0.06	2.90E-04	665.9	10.6

	748	0.17	0.17	1.03	0.07	1.29E-03	777.5	30.0
	773	0.16	0.28	1.78	0.06	1.23E-03	706.9	33.3
VAlO-G-BN	723	0.11	0.19	1.66	0.07	3.58E-04	806.5	5.8
	748	0.14	0.29	2.10	0.06	5.28E-04	713.9	8.6
	773	0.13	0.31	2.37	0.06	2.69E-04	678.6	4.4
VAlO-G-Zn	723	0.09	0.10	1.08	0.08	3.54E-04	943.4	5.7
	748	0.15	0.23	1.50	0.07	3.82E-04	860.2	6.2
	773	0.17	0.27	1.64	0.06	1.39E-04	711.4	2.3
VAlO-G-Sep	723	0.15	0.16	1.07	0.08	1.06E-03	944.9	30.4
	748	0.15	0.28	1.82	0.07	1.03E-03	831.4	35.8
	773	0.14	0.30	2.12	0.07	3.71E-04	819.7	8.4

Effect of the O_2/C_3H_8 molar ratio on conversion. Given the catalytic trends discussed in the previous section, these experiments were done at 723 K. **Table 4** shows the behavior of the catalytic formulations in the oxidation of propane as a function of the O_2/C_3H_8 molar ratio on the conversion of both propane and oxygen. For the vanadium-aluminum mixed oxide, we found that increasing the O_2/C_3H_8 molar ratio increased the conversion of propane from 0.30, $O_2/C_3H_8 = 0.7$, to 0.38, $O_2/C_3H_8 = 2.0$, while the conversion of oxygen decreased at a point where it was no longer the limiting reactant. This trend is reflected on the fact that the ratio of the conversions of the reactants, $X_{O_2}/X_{C_3H_8}$, decreased from 3.4 to ~ 2.0; where the latter has been often reported for catalysts based on vanadium oxides.[32,68,71–73] In contrast, the catalytic formulation done with graphite showed a constant conversion of propane, ca. 0.22, regardless of the O_2/C_3H_8 fed to the reactor. Consequently, in this case, oxygen was not a limiting reactant either. This trend confirms that graphite modifies the reactivity of the vanadium-aluminum mixed oxide.[32,34] After establishing the above facts about the catalysts that serve as comparison bases for assessing the effects of the secondary shaping additives.

The conversion of propane over VAlO-G-Mg was roughly constant and like the one observed for VAlO-G; 0.22±0.02, regardless of the O_2/C_3H_8 molar ratio fed to the reactor.

Therefore, the addition of basic magnesium oxide to the formulation did not change the catalytic reactivity towards the alkane. On the other hand, oxygen was not fully converted under any O_2/C_3H_8 molar ratio and this trend was what made the catalytic behavior of VAlO-G-Mg differ from the behavior of both the VAlO catalytic phase and the VAlO-G formulation. Coming back to the results found for the formulation made with magnesium oxide as a function of temperature, the reader may recall that this was the formulation with the lowest consumption of oxygen overall.

Table 4. Molar fraction conversion of propane and oxygen as a function of the O_2/C_3H_8 molar ratio over particles recovered from tablets of the catalytic formulations. Reaction conditions: U-shaped quartz fixed bed reactor, T = 723 K, *p* = atmospheric pressure (Louvain-la-Neuve ~ 1.03 bar), catalyst weight ~ 0.1 g, average diameters of the catalyst particles 315 – 200 μm, catalytic bed volume ~ 1.0 cm^3 (catalyst plus ca. 0.4 g of quartz spheres of diameter ≤ 200 μm), Total gas flow, F_{Tot} [cm^3/min] = 40. Nomenclature: VAlO = vanadium-aluminum mixed oxide; G = 1.0 wt.% graphite; Mg = magnesium oxide; Si = silica; BN = boron nitride; Zn = zinc oxide; Sep = sepiolite.

Catalyst code	O_2/C_3H_8	$X_{C_3H_8}$	X_{O_2}	$X_{O_2}/X_{C_3H_8}$
VAlO	0.7	0.30	1.00	3.4
	1.0	0.34	0.95	2.8
	1.5	0.34	0.72	2.1
	2.0	0.38	0.87	2.3
VAlO-G	0.7	0.22	0.94	4.2
	1.0	0.22	0.88	4.0
	1.5	0.22	0.41	1.9
	2.0	0.22	0.32	1.4
VAlO-G-Mg	0.7	0.20	0.74	3.7
	1.0	0.21	0.64	3.1
	1.5	0.24	0.65	2.8
	2.0	0.23	0.51	2.2
VAlO-G-Si	0.7	0.27	0.98	3.7
	1.0	0.28	0.93	3.3
	1.5	0.30	0.75	2.5
	2.0	0.35	0.76	2.2
VAlO-G-BN	0.7	0.28	1.00	3.5

	1.0	0.36	1.00	2.8
	1.5	0.39	0.85	2.2
	2.0	0.46	0.81	1.7
VAlO-G-Zn	0.7	0.29	1.00	3.4
	1.0	0.30	0.89	3.0
	1.5	0.32	0.90	2.8
	2.0	0.42	0.94	2.2
VAlO-G-Sep	0.7	0.30	1.00	3.4
	1.0	0.37	0.99	2.7
	1.5	0.51	1.00	2.0
	2.0	0.58	1.00	1.7

In the case of the other formulations, the conversion of propane increased with increasing the O_2/C_3H_8 molar ratio. Besides, these formulations tended to consume all the oxygen supplied to the reaction hence remarking the central role played by surface activated oxygen species on their reactivity towards the alkane. However, as more oxygen was supplied to the reactor, the formulations made with all additives were not able to fully convert it, except for sepiolite. It is interesting to take a closer look at the behavior of the formulation made with sepiolite since, as observed in **Table 4**, it always consumed all the supplied oxygen while steadily increasing the conversion of propane from 0.30, at O_2/C_3H_8 molar ratio = 0.7, to 0.60, at O_2/C_3H_8 molar ratio = 2.0. This is peculiar because for the other formulations the conversion of oxygen decreased by increasing the O_2/C_3H_8 molar ratio. Sepiolite is a clay with a chainlike structure that make mesoporous needlelike particles.[37,74,75] The hydration or dehydration of sepiolite makes its crystals to fold or unfold by the rotation of its Si-O-Si bonds.[75] Such processes indicate that this clay has an important capacity to restructure under reactive atmospheres that contain water vapor. Water vapor is known to modify the catalytic reactivity of vanadium oxide in propane oxidation.[54,76] However, defining the possible effect of water vapor on the catalytic performance falls out of the scope of the present investigation.

Effect of the O_2/C_3H_8 molar ratio on the distribution of products. **Table 5** shows the yield to the reaction products as a function of the O_2/C_3H_8 molar ratio for the different catalytic formulations. In general, the increase of the O_2/C_3H_8 molar ratio favored the total combustion of propane for all formulations except for the one made solely with graphite, VAlO-G. Indeed, only VAlO-G showed a slight increase in the production of propene with the increase of the O_2/C_3H_8 molar ratio. From these results and the ones presented in **Table 4**, one may conclude that the increase in the supply of the oxygen to the reactor led to the production of surface oxygen species that mostly combusted the activated surface hydrocarbons.

Table 5. Molar yields (y_j) from propane oxidation as a function of the O_2/C_3H_8 molar ratio over particles recovered from tablets of the catalytic formulations. Reaction conditions: U-shaped quartz fixed bed reactor, T = 723 K, *p* = atmospheric pressure (Louvain-la-Neuve ~ 1.03 bar), catalyst weight ~ 0.1 g, average diameters of the catalyst particles 315 – 200 μm, catalytic bed volume ~ 1.0 cm^3 (catalyst plus ca. 0.4 g of quartz spheres of diameter ≤ 200 μm), Total gas flow, F_{Tot} [cm^3/min] = 40. Nomenclature: VAlO = vanadium-aluminum mixed oxide; G = 1.0 wt.% graphite; Mg = magnesium oxide; Si = silica; BN = boron nitride; Zn = zinc oxide; Sep = sepiolite. *y_{Oxy} : yield to oxygenated hydrocarbons = sum of the yields of 2-methyloxirane, propanal, 2-propanone, 2-propenal, 1,3,3-triethoxy-1-propene.

Catalyst code	O_2/C_3H_8	y_{CO_2}	y_{CO}	y_{CO}/y_{CO_2}	$y_{C_3H_6}$	y_{oxy}*
VAlO	0.7	0.08	0.09	1.12	0.10	3.22E-03
	1.0	0.07	0.07	0.95	0.07	3.88E-03
	1.5	0.11	0.07	0.59	0.06	2.34E-04
	2.0	0.28	0.03	0.10	0.03	0.00
VAlO-G	0.7	0.12	0.03	0.28	0.05	5.79E-04
	1.0	0.13	0.02	0.13	0.01	4.50E-04
	1.5	0.08	0.02	0.19	0.05	6.60E-03
	2.0	0.09	0.02	0.20	0.05	5.60E-03
VAlO-G-Mg	0.7	0.09	0.02	0.23	0.07	7.11E-04
	1.0	0.10	0.01	0.10	0.03	7.87E-04
	1.5	0.17	0.01	0.05	0.01	0.00
	2.0	0.17	0.01	0.04	0.00	0.00
VAlO-G-Si	0.7	0.08	0.08	0.98	0.07	2.70E-03
	1.0	0.12	0.03	0.30	0.04	6.51E-04
	1.5	0.12	0.05	0.37	0.04	3.54E-03
	2.0	0.17	0.03	0.17	0.04	4.86E-03
VAlO-G-BN	0.7	0.08	0.11	1.35	0.08	3.23E-03

	1.0	0.08	0.11	1.49	0.05	2.86E-03
	1.5	0.13	0.11	0.88	0.05	2.77E-03
	2.0	0.17	0.13	0.76	0.04	0.00
VAlO-G-Zn	0.7	0.09	0.08	0.93	0.09	0.00
	1.0	0.09	0.06	0.67	0.06	0.00
	1.5	0.23	0.02	0.09	0.03	0.00
	2.0	0.31	0.02	0.07	0.02	0.00
VAlO-G-Sep	0.7	0.08	0.12	1.48	0.09	2.99E-03
	1.0	0.08	0.11	1.41	0.06	4.24E-03
	1.5	0.10	0.24	2.28	0.05	2.54E-03
	2.0	0.12	0.32	2.58	0.04	0.00

Considering the ensemble of the catalytic results presented above, we will make a succinct comparison of the performance of the formulations made with boron nitride and sepiolite with the vanadium-aluminum mixed oxide catalytic phase. The comparison will be made in terms of the evolution of the yields to propene, and the CO/CO_2 yield ratio as a function of the conversion of propane, **Figure 4**. For this purpose, we will only consider the results obtained at 723 K. The plots evidence how both boron nitride and sepiolite keep the production of propene at a slightly higher level than the vanadium-aluminum mixed oxide catalytic phase at higher conversions of propane. In addition, while over the VAlO phase the CO/CO_2 yield ratio steeply drops as the conversion of propane increases, over the catalytic formulation made with boron nitride this ratio did decrease so sharply, and, conversely, over the catalytic formulation made with sepiolite the CO/CO_2 yield ratio increased at higher conversions. These trends further demonstrate that both boron nitride and sepiolite contribute individually to the catalytic reactivity of the formulated tablets. The evidence suggests that they may act by modulating the reactivity of the activated surface species and by contributing with their own active sites.

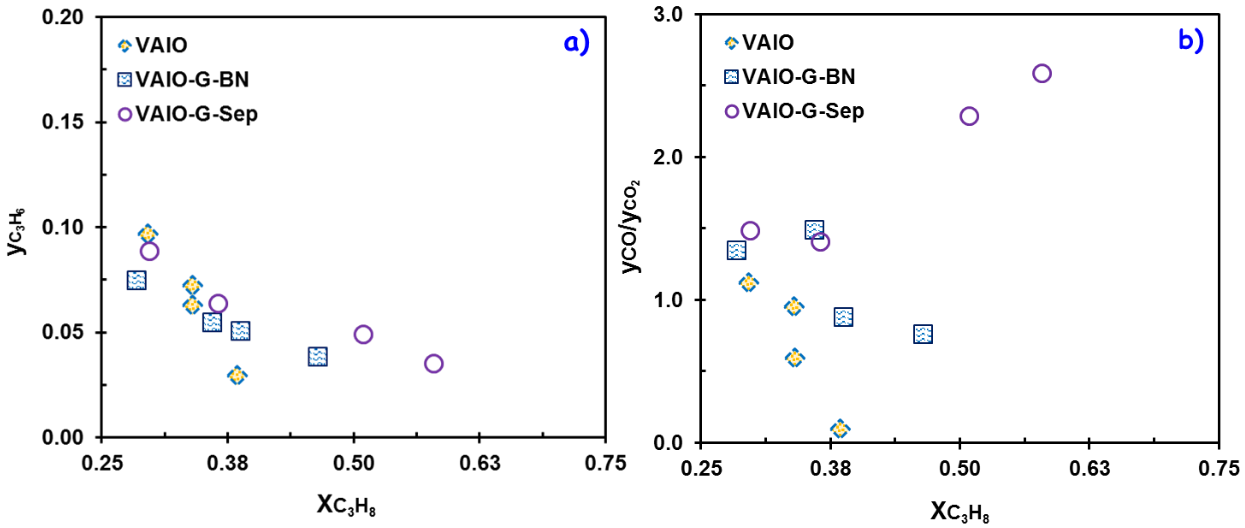

Figure 4. Molar yield to propene ($y_{C_3H_6}$) -**a)**- and y_{CO}/y_{CO_2} ratio -**b)**- from propane oxidation as a function of the conversion of propane ($y_{C_3H_8}$) over particles recovered from tablets of the catalytic formulations: VAlO, VAlO-G-BN, and VAlO-G-Sep. Reaction conditions: U-shaped quartz fixed bed reactor, T = 723 K, *p* = atmospheric pressure (Louvain-la-Neuve ~ 1.03 bar), catalyst weight ~ 0.1 g, average diameters of the catalyst particles 315 – 200 μm, catalytic bed volume ~ 1.0 cm^3 (catalyst plus ca. 0.4 g of quartz spheres of diameter ≤ 200 μm), Total gas flow, F_{Tot} [cm^3/min] = 40. Nomenclature: VAlO = vanadium-aluminum mixed oxide; G = 1.0 wt.% graphite; BN = boron nitride; Sep = sepiolite.

3.3 General considerations

Figure 5 shows boxplots correlating the fractional conversion of propane and the molar yield to CO with the concentration of surface carbon as measured by XPS. In the case of the conversion of propane, the obtained correlation is an apparent volcano plot. The top of the volcano is occupied by the formulation VAlO-G-Sep; i.e. the most reactive catalytic formulation. As we mentioned before, surface carbon measured by XPS may be used as a marker for the acidobasicity of catalytic oxides because metallic oxides minimize their surface energy by adsorbing adventitious carbon.[52] Therefore, the higher the surface free energy of the oxide, the higher its tendency to adsorb hydrocarbons on their lattice. During a catalytic test, the surface free energy of the catalyst is modified by reaction conditions owing to surface restructuring phenomena.[52]

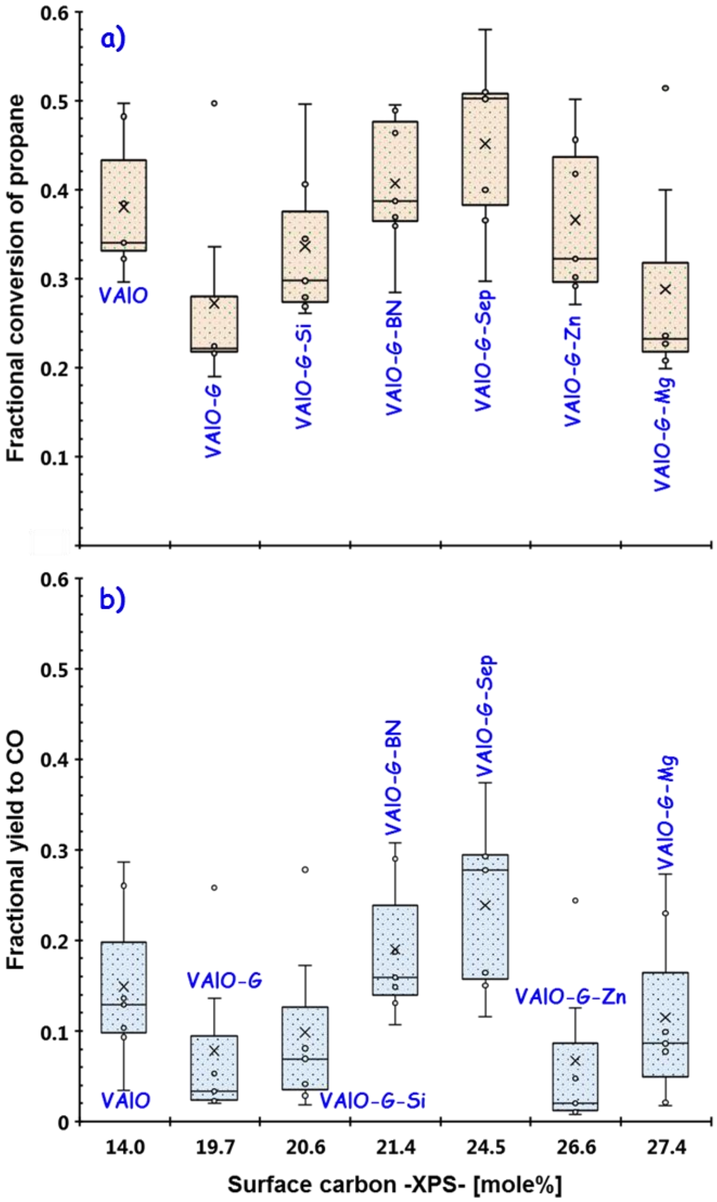

Figure 5. Boxplots correlating the fractional conversion of propane -**a)**- and the molar yield to CO -**b)**- with the concentration of surface carbon as measured by XPS. Reaction conditions: U-shaped quartz fixed bed reactor, T = 723, 748, and 773 K, O_2/C_3H_8 molar ratios = 0.7, 1.0, 1.5, and 2.0, *p* = atmospheric pressure (Louvain-la-Neuve ~ 1.03 bar), catalyst weight ~ 0.1 g, average diameters of the catalyst particles 315 – 200 μm, catalytic bed volume ~ 1.0 cm^3 (catalyst plus ca. 0.4 g of quartz spheres of diameter ≤ 200 μm), Total gas flow, F_{Tot} [cm^3/min] = 40. Nomenclature: VAlO = vanadium-aluminum mixed oxide; G = 1.0 wt.% graphite; Mg = magnesium oxide; Si = silica; BN = boron nitride; Zn = zinc oxide; Sep = sepiolite.

What is interesting from the tendency found in Figure 5 is that it suggests that there is a link between the catalytic reactivity of an oxide in a hydrocarbon oxidation reaction and its affinity towards the adsorption of environmental carbon. The correlation between the production of CO and the concentration of adventitious carbon also showed a volcano shape type trend. However, the relative positions of the different formulations in the plot shifted. Namely, the formulations VAlO, VAlO-G, VAlO-G-Si, VAlO-G-Zn, and VAlO-G-Mg were roughly at the same level in the plot, while VAlO-G-Sep remained at the top closely followed by VAlO-G-BN. The adsorption of adventitious hydrocarbon over a surface makes it hydrophobic.[77,78] As we discussed earlier, under reaction conditions, water vapor may play a role on the catalytic behavior of the formulated materials. Considering these arguments and the correlations found in **Figure 5**, we suggest that the hydrophobicity developed by surface of the formulations VAlO-G-Sep and VAlO-G-BN after reacting with propane may increase the rate of desorption of surface water or modify the reactivity of in-situ formed surface hydroxyls hence slowing the oxidation of CO to CO_2. It is important to say that the above commented correlations were not found for the yields to propene and CO_2, **Figure S6**.

Finally, we correlated the catalytic performance with the V^{5+}/V^{4+} molar ratio measured by XPS, **Figure 6**. Once again, the formulations made with sepiolite and boron nitride made a difference as compared to the other formulations. Particularly, they exhibited the highest propane conversion and CO yield while having the lowest V^{5+}/V^{4+} molar ratios. According to the literature,[68,73,79] the V^{5+}/V^{4+} molar ratio of vanadium oxide based catalysts determines their reactivity and selectivity in hydrocarbon oxidation reactions; where, V^{4+} moieties are thought to favor the production of propene. We could not verify this relationship for the case of the catalytic formulations studied herein since the yield to propene, as well as the yield to CO_2, showed a constant correlation with the V^{5+}/V^{4+} molar ratio of the materials, **Figure S7**. These results further support our previous hypothesis that the present multicomponent catalytic materials react by two simultaneous mechanisms in the oxidation of propane.

Figure 6. Boxplots correlating the fractional conversion of propane -**a)**- and the molar yield to CO -**b)**- with the concentration of surface carbon as measured by XPS. Reaction conditions: U-shaped quartz fixed bed reactor, T = 723, 748, and 773 K, O_2/C_3H_8 molar ratios = 0.7, 1.0, 1.5, and 2.0, *p* = atmospheric pressure (Louvain-la-Neuve ~ 1.03 bar), catalyst weight ~ 0.1 g, average diameters of the catalyst particles 315 – 200 μm, catalytic bed volume ~ 1.0 cm^3 (catalyst plus ca. 0.4 g of quartz spheres of diameter ≤ 200 μm), Total gas flow, F_{Tot} [cm^3/min] = 40. Nomenclature: VAlO = vanadium-aluminum mixed oxide; G = 1.0 wt.% graphite; Mg = magnesium oxide; Si = silica; BN = boron nitride; Zn = zinc oxide; Sep = sepiolite.

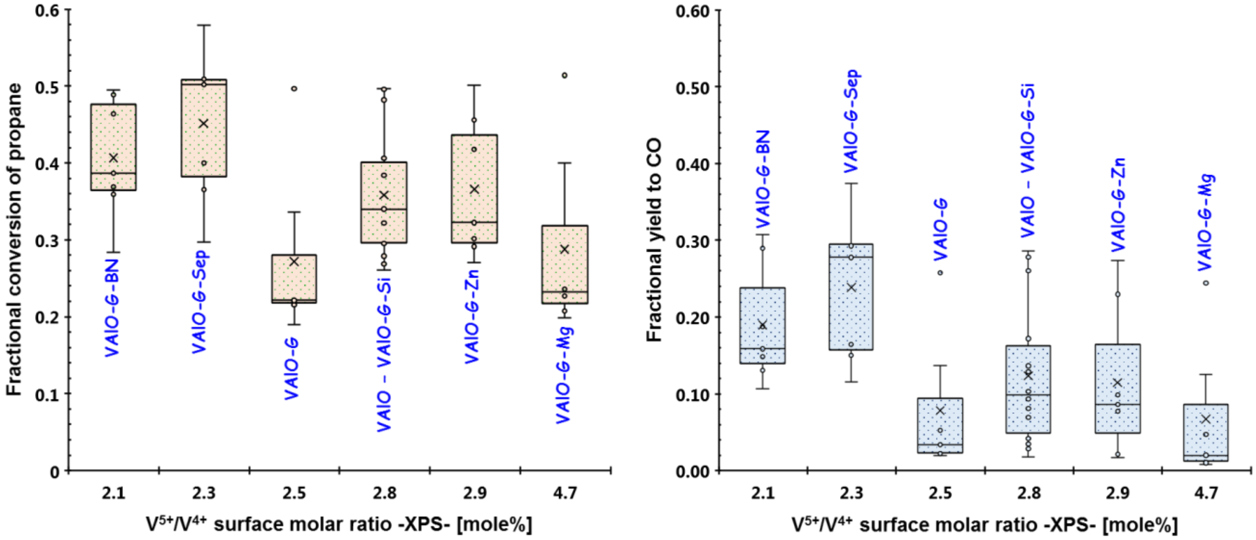

CONCLUSIONS.

Building on our previous investigations concerning the effects of shaping on the properties of catalysts for oxidation reactions, we investigated how secondary additives for tableting vanadium-aluminum mixed-oxides affect the mechanical resistance, surface chemistry, and catalytic performance in propane oxidation. For this purpose, we formulated tablets using 1.0 wt.% graphite as a shaping agent and further added 5.0 wt.% magnesium oxide, silica, boron nitride, sepiolite, and zinc oxide. Our results showed the following: (i) all the tablets formulated with the cited additives had a higher mechanical resistance to axial compression as compared to the tablets made with the vanadium-aluminum mixed oxide powder. However, only those formulated with silica had a stronger mechanical resistance than the ones formulated solely with graphite. In this sense, we found that the changes in mechanical strength were directly related to the softness and ductility of the secondary additive. (ii) All the formulated tablets retained the mesoporous structure of the vanadium-aluminum catalytic phase. However, the formulated tablets had lower surface areas and total pore volumes as compared to the former. These losses depended on the nature of the additives in a similar manner as the mechanical strength did. Therefore, we suggest that there is strong correlation between the softness and ductility of the secondary additives and the modifications in the mechanical strength and the porosity of the catalysts shaped by tableting. (iii) The used secondary additive did not modify the surface chemistry of the vanadium-aluminum mixed oxide but simply mixed mechanically with it during the tableting operation. For this reason, there was no correlation between the measured surface chemistry of vanadium for the different catalytic formulation and their performance in propane oxidation. (iv) Though the additives did not modify the surface chemistry of the catalytic vanadium-aluminum mixed oxide phase, the evidence suggested that they may act as co-catalysts during propane oxidation. Particularly, boron nitride and sepiolite showed the stronger modifications of the catalytic behavior since the formulations made with them were more reactive than the vanadium-aluminum mixed oxide while exhibiting a better productivity of propene. An analysis of the distribution of products obtained with the different catalytic formulations led to suggest that such alterations of the catalytic behavior can be explained by the combination of a redox mechanism over the vanadium-aluminum mixed phase and a surface radical mechanism occurring over the active moieties of the secondary additives.

ASSOCIATED CONTENT

The Supporting Information is available free of charge. It includes: Data on mechanical resistance, surface chemistry by XPS, N_2 physisorption characterization and surface area and porosity calculations, and catalytic data.

AUTHOR INFORMATION

Corresponding Authors

*Eric M. Gaigneaux - Institute of Condensed Matter and Nanosciences (IMCN), Division Molecular Chemistry, Materials and Catalysis (MOST), UCLouvain, Place Louis Pasteur 1, box L4.01.09, B-1348 Louvain-la-Neuve, Belgium; https://orcid.org/0000-0003-2239-4306; email: eric.gaigneaux@uclouvain.be.

*Víctor Gabriel Baldovino-Medrano − Centro de Investigaciones en Catálisis (CICAT) and Laboratorio de Ciencia de Superficies (SurfLab), Parque Tecnológico de Guatiguará, km 2 vía El Refugio, Universidad Industrial de Santander, Piedecuesta (Santander), 681011, Colombia; https://orcid.org/0000-0003-3227-0251; email: vicbaldo@uis.edu.co; Tel.: +57 6344000; Ext: 1485; 3485. Twitter: @vigabalme.

Author Contributions

The manuscript was written through contributions of all authors. All authors have given approval to the final version of the manuscript.

Funding Sources

This work was done within the Frame of the IAP P6/17 “Inanomat” project entitled “Advanced complex inorganic materials by a novel bottom-up nanochemistry approach: processing and shaping”.

ACKNOWLEDGMENT

V.G.B.-M. thanks the office of the “Politique scientifique fédérale belge” for a postdoctorate fellowship. The authors thank Michel Genet, Marc Sinnaeve, and Pascal Valvassori for their help in making the experiments featured in this work.

REFERENCES

(1) Stillwell, W. D. *Preformed Catalysts and Techniques of Tableting*. Ind. Eng. Chem. 1957, 49 (2), 245–249.

(2) Berrebi, G., Bernusset, P. *Making Industrial Catalysts,* Stud. Surf. Sci. Catal. **1976**, 1, 13–38.

(3) Bartholomew, C. H.; Farrauto, R. J. *Fundamentals of Industrial Catalytic Processes*, 2nd ed.; John Wiley & Sons, Inc.: Hoboken, New Jersey, **2006**.

(4) Schüth, F.; Hesse, M. *Catalyst Forming. In Handbook of heterogeneous catalysis*; Ertl, G., Knözinger, H., Schüth, F., Weitkamp, J., Eds.; Wiley-VCH Verlag GmbH& Co. KGaA: Weinheim, **2008**; p 3865.

(5) Kraushaar-Czarnetzki, B.; Muller, P. S. *Shaping of Solid Catalysts. In Synthesis of solid catalysts*; de Jong, K. P., Ed.; Wiley-VCH Verlag GmbH & Co. KGaA: Weinheim, **2009**; p 26.

(6) Birtill, J. J. *Some Experiences in Industrial Catalysis*. J. Mol. Catal. A Chem. 2009, 305 (1–2), 183–189.

(7) Mitchell, S.; Michels, N.-L.; Pérez-Ramírez, J. *From Powder to Technical Body: The Undervalued Science of Catalyst Scale Up*. Chem. Soc. Rev. **2013**, 42 (14), 6094–6112.

(8) Bingre, R., Louis, B., Nguyen, P. *An Overview on Zeolite Shaping Technology and Solutions to Overcome Diffusion Limitations,* Catalysts **2018**, 8, 1-18.

(9) Le Page, J.F., Miquel, J. *Determining Mechanical Properties of Industrial Catalysts: Correlations With Their Morphological and Physical-Chemical Properties,* Stud. Surf. Sci. Catal. **1976**, 1, 39–50.

(10) Areshidze, K.I., Chivadze, G.O. *Effects of Different Factors on the Specific Surface Area, Activity, Stability and Mechanical Strength of Industrial Catalysts,* Stud. Surf. Sci. Catal. **1976**, 1, 559–567.

(11) Le Page, J. -F., Cosyns, J., Courty, P., Freund, E., Franck, J.-P., Jacquin, Y., Juguin, B., Marcilly, C., Martino, G., Miquel, J., Montarnal, R., Sugier, A., Van Landeghem, H. *Applied heterogeneous catalysis: design, manufacture, use of solid catalysts,* 1st ed., Institut Français du Petrole, Paris, **1987**.

(12) Satterfield, C. N. *Heterogeneous Catalysis in Industrial Practice*, 2nd ed.; Krieger Publishing company: Malabar, **1991**.

(13) Stiles, A. B.; Koch, T. A. *Catalyst Manufacture*, 2nd ed.; CRC Press: Boca Raton, **1995**.

(14) Perego, C.; Villa, P. *Catalyst Preparation Methods*. Catal. Today **1997**, 34 (3), 281–305.

(15) Font Freide, J. J. H. M.; Gamlin, T. D.; Graham, C.; Hensman, J. R.; Nay, B.; Sharp, C. *An Adventure in Catalysis: The Story of the BP Fischer–Tropsch Catalyst from Laboratory to Full-Scale Demonstration in Alaska*. Top. Catal. **2003**, 26 (1), 3–12.

(16) Armor, J. N. *Do You Really Have a Better Catalyst?* Appl. Catal. A Gen. **2005**, 282 (1), 1–4.

(17) Campanati, M.; Fornasari, G.; Vaccari, A. *Fundamentals in the Preparation of Heterogeneous Catalysts*. Catal. Today **2003**, 77 (4), 299–314.

(18) Johansen, K. *Aspects of scale-up of catalyst production*, Stud. Surf. Sci. Catal. **2000**, 143, 1–15.

(19) Froment, G.; Bischoff, K. B.; De Wilde, J. *Chemical Reactor - Analysis and Design*, 3rd ed.; John Wiley & Sons: New York, **2011**.

(20) Larsson, A.-C. *Study of Catalyst Deactivation in Three Different Industrial Processes*, PhD Thesis, Växjö University, **2007**.

http://www.diva-portal.org/smash/record.jsf?pid=diva2%3A204839&dswid=3907.

(21) Duarte, L., Garzón, L., Baldovino-Medrano, V.G. *An analysis of the physicochemical properties of spent catalysts from an industrial hydrotreating unit*, Catal. Today. **2019**, 338, 100-107.

(22) Couroyer, C.; Ghadiri, M.; Laval, P.; Brunard, N.; Kolenda, F. *Methodology for Investigating the Mechanical Strength of Reforming Catalyst Beads*. Oil Gas Sci. Technol. - Rev. IFP **2000**, 55 (1), 67–85.

(23) Spatenka, S.; Matzopoulos, M.; Urban, Z.; Cano, A. *From Laboratory to Industrial Operation: Model-Based Digital Design and Optimization of Fixed-Bed Catalytic Reactors*. Ind. Eng. Chem. Res. **2019**, 58 (28), 12571–12585.

(24) Butt, J.; Petersen, E. E. *Activation, Deactivation, and Poisoning of Catalysts*, 1st ed.; Elsevier Inc.: Amsterdam, **1988**.

(25) Torres-Mancera, P.; Rayo, P.; Ancheyta, J.; Marroquín, G.; Centeno, G.; Alonso, F. *Catalyst Deactivation Pattern along a Residue Hydrotreating Bench-Scale Reactor*. Catal. Today **2014**, 220–222, 153–158.

(26) Rodríguez, E.; Félix, G.; Ancheyta, J.; Trejo, F. *Modeling of Hydrotreating Catalyst Deactivation for Heavy Oil Hydrocarbons*. Fuel **2018**, 225, 118–133.

(27) Rao, S. M.; Coppens, M.-O. *Mitigating Deactivation Effects through Rational Design of Hierarchically Structured Catalysts: Application to Hydrodemetalation*. Ind. Eng. Chem. Res. **2010**, 49 (21), 11087–11097.

(28) Zakeri, M.; Samimi, A.; Afarani, M. S.; Salehirad, A. *Interaction between Weibull Parameters and Mechanical Strength Reliability of Industrial-Scale Water Gas Shift Catalysts*. Particuology **2017**, 32, 160–166.

(29) Zakeri, M., Samimi, A., Khorram, M., Atashi, H., Mirzaei, A. *Effect of forming on selectivity and attrition of co-precipitated Co–Mn Fischer–Tropsch catalysts*, Powder Technol. **2010**, 200, 164–170.

(30) Thon, A., Werther, J. *Attrition resistance of a VPO catalyst*, Appl. Catal. A Gen. **2010**, 376, 56–65.

(31) Baldovino-Medrano, V.G., Le, M.T., Van Driessche, I., Bruneel, E., Gaigneaux, E.M. *Influence of graphite as a shaping agent of Bi molybdate powders on their mechanical, physicochemical, and catalytic properties*, Ind. Eng. Chem. Res. **2011**, 50, 5467–5477.

(32) Baldovino-Medrano, V.G., Farin, B., Gaigneaux, E.M., *Establishing the role of graphite as a shaping agent of vanadium-aluminum mixed (Hydr)oxides and their physicochemical properties and catalytic functionalities*, ACS Catal. **2012**, 2, 322–336.

(33) Baldovino-Medrano, V.G., Alcázar, C., Colomer, M.T., Moreno, R., Gaigneaux, E.M. *Understanding the molecular basics behind catalyst shaping: Preparation of suspensions of vanadium-aluminum mixed (hydr)oxides*, Appl. Catal. A Gen. **2013**, 468, 190-213.

(34) Baldovino-Medrano, V.G., Le, M.T., Van Driessche, I., Bruneel, E., Alcázar, C., Colomer, M.T., Moreno, R., Florencie, A., Farin, B., Gaigneaux, E.M. *Role of shaping in the preparation of heterogeneous catalysts: Tableting and slip-casting of oxidation catalysts*, Catal. Today **2015**, 246, 81-91.

(35) Baldovino-Medrano, V.G., Kartheuser, B., Gaigneaux, E.M. *Production and testing of technical catalysts based on MnO_2 for the abatement of aromatic volatile compounds at the laboratory and pilot plant scales*, Catal. Today. **2019**, 338, 81–92.

(36) Baldovino-Medrano, V.G., Farin, B., Gaigneaux, E.M., *Understanding the role of shaping on the performance of oxidation catalysts: Analysis of the effect of tableting additives for vanadium-aluminium mixed oxides*, in: Proc. 7th World Conf. Oxid. Catal., Saint Luois, 2013. http://catalysisclubphilly.org/news/seventh-world-congress-on-oxidation-catalysis/.

(37) Corma, A., Perez-Pariente, J., Fornes, V., Mifsud, A. *Surface acidity and catalytic activity of a modified sepiolite*, Clay Miner. **1984**, 19, 673–676.

(38) Blangenois, N., Florea, M., Grange, P., Silvy, R.P., Chenakin, S.P., Bastin, J.M., Kruse, N., Barbero, B.P., Cadús, L. *Influence of the co-precipitation pH on the physico-chemical and catalytic properties of vanadium aluminum oxide catalyst*, Appl. Catal. A Gen. **2004**, 263, 163–170.

(39) Silvy, R.P., Blangenois, N., Hamrouni, M., Grange, P., Gaigneaux, E.M. *Parameters controlling the scaling-up of a V-Al oxynitride catalyst for the ammoxidation of propane*, Stud. Surf. Sci. Catal. **2006**, 162, 187–194.

(40) Baldovino-Medrano, V.G., Pollefeyt, G., Bliznuk, V., Van Driessche, I., Gaigneaux, E.M., Ruiz, P., Wojcieszak, R. *Synergetic Behavior of TiO_2-Supported Pd(z)Pt(1-z) Catalysts in the Green Synthesis of Methyl Formate*, ChemCatChem. **2016**, 8, 1157-1166.

(41) Baldovino-Medrano, V.G., Ospina, R., Gaigneaux, E.M. *Differential charging effects from impurities in pyrolytic graphite*, Appl. Surf. Sci. **2019**, 476, 174–181.

(42) Lide, D.R. *CRC Handbook of Chemistry and Physics*, 90th ed., CRC Press/Taylor and Francis, Boca Raton, **2010**.

(43) Andrew, S.P.S. *Theory and practice of the formulation of heterogeneous catalysts*, Chem. Eng. Sci. **1981**, 36, 1431–1445.

(44) Condon, J.B. *Surface Area and Porosity Determinations by Physisorption Measurements and Theory*, 1st ed., Elsevier Science, Amsterdam, **2006**.

(45) Condon, J.B., Chi Representation of Standard Nitrogen, Argon, and Oxygen Adsorption Curves, Langmuir. **2001**, 17, 3423–3430.

(46) Brunauer, S., Emmett, P.H., Teller, E. *Adsorption of Gases in Multimolecular Layers*, J. Am. Chem. Soc. **1938**, 60, 309–319.

(47) Barrett, E.P., Joyner, L.G., Halenda, P.P. *The Determination of Pore Volume and Area Distributions in Porous Substances. I. Computations from Nitrogen Isotherms*, J. Am. Chem. Soc. **1951**, 73, 373–380.

(48) Chenakin, S. P.; Silvy, R. P.; Kruse, N. *X-Ray Induced Surface Modification of Aluminovanadate Oxide*. Catal. Letters **2005**, 102 (1), 39–43.

(49) Wagner, C.D. *Studies of the charging of insulators in ESCA*, J. Electron Spectros. Relat. Phenomena. **1980**, 18, 345–349.

(50) Barr, T.L., Seal, S. *Nature of the use of adventitious carbon as a binding energy standard*, J. Vac. Sci. Technol. A. **1995**, 13, 1239–1246.

(51) Johansson, G., Hedman, J., Berndtsson, A., Klasson, M., Nilsson, R. *Calibration of electron spectra*, J. Electron Spectros. Relat. Phenomena. **1973**, 2, 295–317.

(52) Somorjai, G.A., Li, Y. *Introduction to Surface Chemistry and Catalysis*, 2nd ed., John Wiley & Sons, Inc., Hoboken, New Jersey, 2010.

(53) Barthelmy, D. Sepiolite Mineral Data, Mineral. Database. (n.d.). http://www.webmineral.com/data/Sepiolite.shtml (accessed May 24, 2020).

(54) Chen, K., Bell, A.T., Iglesia, E. *Kinetics and Mechanism of Oxidative Dehydrogenation of Propane on Vanadium, Molybdenum, and Tungsten Oxides*, J. Phys. Chem. B. **2000**,104, 1292–1299.

(55) Corma, A., Nieto, J.M.L., Parades, N., Dejoz, A., Vazquez, I. *Oxidative dehydrogenation of propane and n-butane on V-Mg based catalysts*, Stud. Surf. Sci. Catal. **1994**, 82, 113–123.

(56) Corma, A., Nieto, J.M.L., Paredes, N., Pérez, M. *Oxidative dehydrogenation of propane on vanadium supported on magnesium silicates*, Appl. Catal. A Gen. **1993**, 97, 159–175.

(57) Corma, A., Nieto, J.M.L., Paredes, N., *Influence of the Preparation Methods of V-Mg-O Catalysts on Their Catalytic Properties for the Oxidative Dehydrogenation of Propane*, J. Catal. **1993**, 144, 425–438.

(58) Corma, A., Nieto, J.M.L., Paredes, N., Pérez, M., Shen, Y., Cao, H., Suib, S.L. *Oxidative Dehydrogenation Of Propane Over Supported-Vanadium Oxide Catalysts*, Stud. Surf. Sci. Catal. **1992**, 72, 213–220.

(59) Grant, J.T., Carrero, C.A., Goeltl, F., Venegas, J., Mueller, P., Burt, S.P., Specht, S.E., McDermott, W.P., Chieregato, A., Hermans, I. *Selective oxidative dehydrogenation of propane to propene using boron nitride catalysts*, Science **2016**, 354, 1570-1573.

(60) Venegas, J.M., McDermott, W.P., Hermans, I. *Serendipity in Catalysis Research: Boron-Based Materials for Alkane Oxidative Dehydrogenation*, Acc. Chem. Res. **2018**, 51 2556–2564.

(61) Love, A.M., Thomas, B., Specht, S.E., Hanrahan, M.P., Venegas, J.M., Burt, S.P., Grant, J.T., Cendejas, M.C., McDermott, W.P., Rossini, A.J., Hermans, I. *Probing the Transformation of Boron Nitride Catalysts under Oxidative Dehydrogenation Conditions*, J. Am. Chem. Soc. **2019**, 141, 182–190.

(62) Delmon, B., Froment, G.F. *Remote Control of Catalytic Sites by Spillover Species: A Chemical Reaction Engineering Approach*, Catal. Rev. **1996**, 38, 69–100.

(63) B. Delmon, *Are Solid Catalysts Successfully Emulating Enzymes?*, Chinese J. Catal. **2010**, 31, 859–871.

(64) Moro-Oka, Y. *Oxygen spillover for the design of industrial oxidation catalysts*, Stud. Surf. Sci. Catal. **1993**, 77, 95–103.

(65) Delmon, B. *Solid-State Reactions in Catalysts During Ageing: Beneficial Role of Spillover*, Stud. Surf. Sci. Catal. **1994**, 88, 113–128.

(66) Vayenas, C., Brosda, S. *Spillover-modified catalysis: Experimental rules and mathematical modeling*, Stud. Surf. Sci. Catal. **2001**, 138, 197–204.

(67) Vuong, H., Binder, A.J., Sutton, J.E., Toops, T., Savara, A. *Experimental data based combinatorial kinetic simulations for predictions of synergistic catalyst mixtures*, Catal. Today **2019**, 338, 117–127.

(68) Albonetti, S.; Cavani, F.; Trifirò, F. *Key Aspects of Catalyst Design for the Selective Oxidation of Paraffins*. Catal. Rev. **1996**, 38 (4), 413–438.

(69) Dria, D. E.; Bremer, N. J. *Process for Tableting Fine Powders*. US Patent 4426342, **1984**.

(70) Buyevskaya, O.V., Baerns, M. *Catalytic selective oxidation of propane*, Catal. Today **1998**, 42, 315–323.

(71) Hernández-Maya, M.S., Espinosa-Lobo, C.B., Cabanzo-Hernández, R, .Mejía-Ospino, E., Baldovino-Medrano, V.G. *Propane oxidation over silica supported sodium vanadate catalysts*, ACS Catal. **2020**, *Under review*.

(72) Cavani, F., Trifirò, F. *The oxidative dehydrogenation of ethane and propane as an alternative way for the production of light olefins*, Catal. Today **1995**, 24, 307–313.

(73) Cavani, F., Ballarini, N., Cericola, A. *Oxidative dehydrogenation of ethane and propane: How far from commercial implementation?,* Catal. Today **2007**, 127, 113–131.

(74) Busca, G. *Bases and Basic Materials in Industrial and Environmental Chemistry: A Review of Commercial Processes*, Ind. Eng. Chem. Res. **2009**, 48, 6486–6511.

(75) Serna, C., Ahlrichs, J.L., Serratosa, J.M. *Folding in Sepiolite Crystals*, Clays Clay Miner. **1975**, 23, 452–457.

(75) Chen, K., Khodakov, A., Yang, J., Bell, A.T., Iglesia, E. *Isotopic Tracer and Kinetic Studies of Oxidative Dehydrogenation Pathways on Vanadium Oxide Catalysts*, J. Catal. 1999, 186, 325–333.

(77) Landoulsi, J.; Genet, M. J.; Fleith, S.; Touré, Y.; Liascukiene, I.; Méthivier, C.; Rouxhet, P. G. *Organic Adlayer on Inorganic Materials: XPS Analysis Selectivity to Cope with Adventitious Contamination*. Appl. Surf. Sci. **2016**, 383, 71–83.

(78) Landoulsi, J.; Genet, M. J.; Richard, C.; El Kirat, K.; Pulvin, S.; Rouxhet, P. G. *Evolution of the Passive Film and Organic Constituents at the Surface of Stainless Steel Immersed in Fresh Water*. J. Colloid Interface Sci. **2008**, 318 (2), 278–289.

(79) Mamedov, E. A.; Cortés Corberán, V. *Oxidative Dehydrogenation of Lower Alkanes on Vanadium Oxide-Based Catalysts. The Present State of the Art and Outlooks*. Appl. Catal. A Gen. **1995**, 127 (1), 1–40.